

Activated boron nitride nanotubes: A potential material for room-temperature hydrogen storage

Seung-Hoon Jhi*

Department of Physics, Pohang University of Science and Technology, Hyojadong San 31, Pohang 790-784, Korea

(Received 4 June 2006; revised manuscript received 2 September 2006; published 20 October 2006)

Activated forms of boron nitride nanotubes are studied for potential applications to hydrogen storage with the use of pseudopotential density functional method. The binding and diffusion energies of adsorbed hydrogen are particularly calculated. The calculated binding energy of hydrogen on activated boron nitride nanotubes is found to lie in the right range for room-temperature storage. It is also shown that diffusion through the active sites enables hydrogen to access the inner surface of the nanotubes, which leads to the increase of the storage capacity. Current study provides a tangible solution to increase the operating temperature and capacity of hydrogen storage based on heteropolar nanomaterials such as boron nitride nanotubes.

DOI: [10.1103/PhysRevB.74.155424](https://doi.org/10.1103/PhysRevB.74.155424)

PACS number(s): 68.43.Bc, 81.07.De, 84.60.Ve

I. INTRODUCTION

Hydrogen is considered as an ideal and clean alternative energy medium replacing current fossil fuels. Among many technical and scientific challenges faced by full hydrogen usage, the development of proper storage systems is one of the most immanent problems awaiting solutions. Nanostructured form of materials has been a main focus in recent hydrogen storage research (Refs. 1 and 2, and references therein). Materials at nanoscales can have advantages over their bulk counterparts with respect to molecular adsorptions such as large specific surface area (SSA) and potentially high binding energy. Nanotubes, nanohorns, and nanoclusters have been tested as possible forms of materials that can enhance the capacity with proper release temperature.³⁻⁷ Unfortunately, nanostructure by itself does not necessarily lead to such expected consequences. Single-walled carbon nanotubes, for example, have been of great interest for their structures of large SSA and curvature. It is now believed that their storage capacity at ambient conditions does not show a significant improvement from that of activated carbons,⁸⁻¹¹ not to mention achieving the target set by the US DOE. A critical flaw in carbon-based nanomaterials is the too weak binding strength of hydrogen. For storage materials operating at near room temperature, the binding energy of hydrogen should be in the range of 0.2–0.5 eV, which is addressed by the van 't Hoff equation.¹² It has been unclear of how to obtain the optimal binding energy without degrading storage capacity as observed in metal-decorated carbon materials. Changing the chemistry or structure of chosen materials has been tested to develop storage systems to meet the target. Recently, the tubular form of boron nitride has been shown to store hydrogen at elevated temperatures compared with carbon nanotube (CNT).¹³⁻¹⁵ Although its SSA ($\sim 200 \text{ m}^2/\text{g}$) was well below that of CNT and activated carbons,^{14,15} it demonstrated a possibility of designing materials with appropriate hydrogen binding properties. Increasing the SSA and binding strength is a next step toward optimizing the tubular structure of boron nitride. Adopting activation processes developed for carbons, for example, can provide a solution of increasing the capacity and release temperatures of nanostructures.

In this paper, activated forms of boron nitride nanotubes (aBNTs) are proposed to reach the optimal hydrogen binding

energy, which is a strong signature that the materials can be a good candidate for room-temperature hydrogen storages. The adsorption property of hydrogen is particularly studied on the activated nanotubes through *ab initio* simulations. We focus on pore structures with various chemicals at their edge as a form of activation. Similar structures in glassy materials have shown to be important for hydrogen adsorption and diffusion.¹⁶ Creating such pore structures of various size and with various atomic edges can be a possible way of activation of BNTs. Accessibility into inner space of the nanotubes is also critical to increase the surface area and the binding energy. The estimation of the diffusion barrier through large-size pores can provide information of their optimal size.

II. COMPUTATIONAL DETAILS

For emulating the local chemistry and structure of pores typically observed in activated carbons, we generate pores in BNTs by removing boron and nitrogen atoms, and then saturate or substitute neighboring atoms by hydrogen, carbon, or oxygen. The saturation is only done for hydrogen by attaching it to neighboring boron and nitrogen atoms. These atoms are commonly observed to make chemical bonding with boron and nitrogen, and advantageous to storage capacity because they are also light elements. We choose a (10,0) zigzag-type tube for the study, and the overall binding properties of hydrogen is believed to be insensitive to the tube types because of the physisorption nature of the binding. Figure 1 shows a schematic view of an (10,0) boron nitride nanotube activated by such processes. The active sites with oxygen are believed to be similar to the oxygenated edges structures in activated carbons. They also resemble the pore structures found in B_2O_3 (Ref. 16) or macrocyclic polyether molecules known as crown ethers.¹⁷⁻¹⁹ In this configuration, boron or nitrogen atoms neighboring the vacancy are substituted by oxygen to form boron-oxygen- or nitrogen-oxygen-bonded edge structures in the vacancy. For example, the active sites illustrated in Fig. 1(a) are generated by removing three boron and one nitrogen atoms and then by substituting the neighboring nitrogen atoms by oxygen. The B-O bonds form the edge of the pore, which looks similar to those found in B_2O_3 . The size of pores can be controlled by changing the number of B and N atoms being removed.

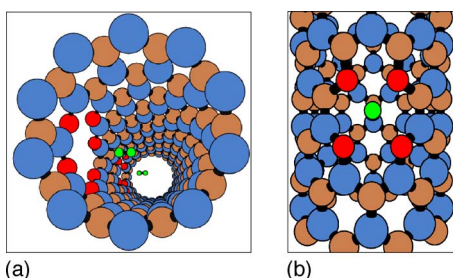


FIG. 1. (Color online) An illustrative view of a (10,0) BNT activated with oxygen-edged vacancies. (a) Top view of the activated nanotube with quadruple vacancies with six oxygen atoms at the edge and (b) side view of the tube with a double-vacancy passivated by four oxygen atoms. A similar chemical activation is also tested for carbon, which substitutes for boron or nitrogen atoms neighboring the vacancy. For testing hydrogen saturation, hydrogen atoms are attached to the boron and nitrogen atoms neighboring the vacancy instead of substituting those atoms. In order to calculate the binding energy of hydrogen molecule on the active sites, hydrogen molecules (denoted by green circles) are put (a) inside the tube or (b) on top of the pore. Red, blue, and dark yellow circles denote oxygen, boron, and nitrogen atoms, respectively.

In order to investigate the binding of hydrogen on activated BNTs, a hydrogen molecule is put on top of the active sites and a series of total energy calculations are performed with the use of the pseudopotential density functional method.^{20,21} Exchange-correlation of electrons is treated within the scheme of the generalized gradient approximation (GGA) developed by Perdew, Burke, and Ernzerhof.²² We note that the physisorption energy with GGA [or with local density approximation (LDA)] usually have large error bars. A recent quantum Monte Carlo calculation²³ shows that the binding energy of hydrogen in carbon materials is in between the GGA and the LDA values. In previous studies, the binding energy calculated with the same computational scheme agrees reasonably well with experiment,^{13,24} and the results presented here can be understood as a reference within a given frame of computational methods. For comparison, the LDA is also used to check the consistency of the trend obtained with GGA. Atomic orbitals with double zeta polarization are used to expand single-particle wave functions²¹ with a cutoff energy of 80 Ry for real space mesh construction. Binding energy curves are obtained by performing successive calculations of total energy at varying distance between the hydrogen molecule and the adsorbent. Full relaxations of atomic positions are carried out with the center of mass of hydrogen being fixed until their Hellmann-Feynman forces are less than 0.01 eV/Å.

III. RESULTS AND DISCUSSIONS

The bond length of B-O and N-O bonds in activated BNTs are found to be about 1.38 and 1.46 Å, respectively. The B-O bond length is close to that in B₂O₃ while the N-O bond length is larger than both single- and double-bonded N-O. For nonpassivated edges or for the passivation with hydrogen or carbon, there is a substantial reconstruction in the active sites. For double-vacancy pores without edge pas-

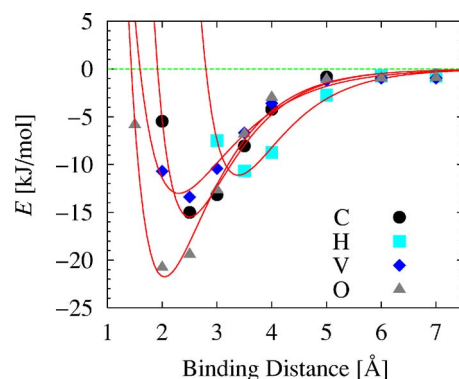


FIG. 2. (Color online) The hydrogen binding energy curves on an activated (10,0) BNT with various types of passivation of vacancies that are generated by removing boron-nitrogen pairs from the tube. The largest binding energy is obtained for oxygen-passivated vacancy pores (filled triangles). Carbon and hydrogen passivations are denoted by filled circles and squares, respectively. The binding energy curve without any passivation (filled diamond) is also plotted for comparison.

sivation, B-B and N-N bonds are formed with a bond length of about 1.75 and 1.48 Å, respectively. And they lead to the formation of pentagon-octagon-pentagon (5-8-5) defect structure in the tube as observed in CNT and graphite with double-vacancy defects.²⁵ Similar defect structures are also observed for carbon-edged double-vacancy pores in the BNT. The C-C bond length, in this case, is about 1.40 Å, which is shorter than B-N bond length by about 4% leading to radial deformations of the tube. On the other hand, the bond length of hydrogen molecule does not change upon adsorption. It is interesting to note that there is a small charge transfer from nanotube to hydrogen of about 0.04 electron/H₂. This implies that the hydrogen adsorption on the activated nanotubes may not be of simple van der Waals type.

Figure 2 shows the binding energy curves of hydrogen on the active sites of BNT with various types of passivation. Hydrogen, carbon, and oxygen atoms were tested for the passivation as described above. The pore was created by removing a single B-N bond from the tube with four neighboring B and N atoms passivated by the chosen atoms [Fig. 1(b)]. As Fig. 2 shows, the most active pore with respect to hydrogen binding is the one passivated by oxygen, giving a binding energy of about 22 kJ/mol. The pores passivated by hydrogen have the smallest binding energy of about 11 kJ/mol, but it is still significantly larger than that on graphite or pure carbon nanotubes of about 6 kJ/mol.²⁶⁻²⁸ The pores without passivation or passivated by carbon have also relatively large binding energies of about 15 kJ/mol. Both types of pores undergo a reconstruction to 5-8-5 structural defects as mentioned above. The calculated results indicate that such substantial structural defects can also enhance the binding energy.¹³ The strong binding of hydrogen on oxygen-passivated pores is probably due to an extended charge distribution of lone-pair electrons in B-O and N-O bonds compared to those formed by H or C with B and N. Similar effects were also observed in boron oxides, where large binding energies were obtained on top of pores that

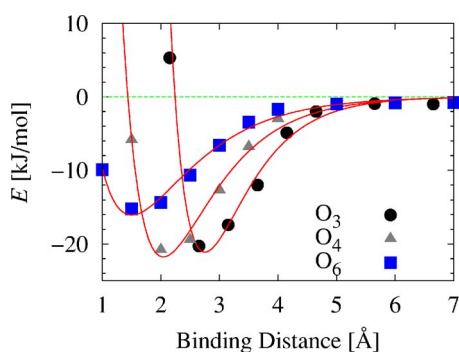


FIG. 3. (Color online) The hydrogen binding energy curves on an activated (10,0) boron nitride nanotube with different size of vacancy pores of single, double, and quadruple vacancies. All of them are passivated by oxygen. The subscript n in O_n denotes the number of oxygen atoms used for the passivation.

have oxygen in the edge.¹⁶ Calculated binding energies are so significant that the desorption temperature (or operating temperature of hydrogen storages) could reach as high as about 210 K as estimated from the van't Hoff equation,¹² which is a significant improvement from both pure BNT and CNT.¹³ From previous calculations of hydrogen binding on similar structured materials, it was shown that the energy depends on the size of the pores on which the hydrogen is adsorbed. The optimal pore size was estimated to be about 6.5 Å.^{16,19}

The binding of hydrogen on BNT is in nature a physisorption type, and it is expected that the binding energy is sensitive to the contact area of hydrogen with the BNT. The large contact area, in other words, means an enhanced overlap of electron charge distribution between hydrogen and the atoms at the pores, which results in bigger exchange-correlation energies and thus in larger binding energies. The size of pores can thus be a controlling parameter of the contact area as the number of atoms in contact with hydrogen apart by the van der Waals distance changes at varying pore size. A caveat is that this argument should be understood within current DFT calculation schemes. Single, double, and quadruple vacancies are generated and then the neighboring atoms are substituted by oxygen. Hydrogen adsorption is simulated in a similar way as described above. Figure 3 shows the calculated binding energy curves of hydrogen on the oxygen-edge pores. It was found that the binding energy is the maximum for the double-vacancy pore that reaches as much as 22 kJ/mol. As the pore size increases, the binding energy is a little reduced, and the binding distance decreases to 1.5 Å for the quadruple-vacancy pore.

We can expect that hydrogen can diffuse into the nanotubes if the pore size is sufficiently larger than the size of hydrogen molecule. In order to study the hydrogen diffusion into the tube, the simulation of hydrogen binding is carried out for quadruple-vacancy pores while decreasing further the distance between the tube and hydrogen molecule. Figure 4 shows the results of the simulation, where the negative distances indicate the hydrogen molecule lying inside the tube. The diffusion barrier is estimated to be about 30 kJ/mol for the quadruple-vacancy pore. The barrier height is strongly correlated with the pore size. The diameter of the pore in this

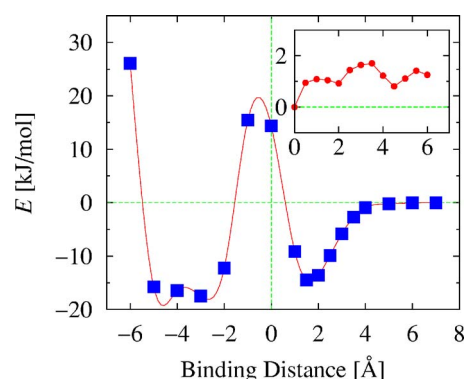


FIG. 4. (Color online) The binding energy curve of hydrogen on top of and also through a pore that has six oxygens in its edge. The solid line is a guide to eye. The distance of 0 Å means that hydrogen is located right at the center of the pore. The negative binding distance indicates that hydrogen is inside the tube that has a diameter of about 8 Å. The energy barrier for hydrogen diffusion is estimated to be about 30 kJ/mol. A slight larger binding energy of hydrogen inside the tube is due to the enhanced contact area. The activated BNTs act as double-welled potentials for hydrogen adsorption. The inset shows the energy variation of hydrogen binding on the inner surface of the tube (in kJ/mol unit). The distance along the tube axis (in Å unit) is given in reference to the center of the pore. This energy corrugation provides an estimate of hydrogen diffusion-energy along the inside of the tube.

calculation is about 5 Å, which is smaller than the optimal pore size for hydrogen diffusion as estimated from B_2O_3 and crown ethers.^{16,19} Using the Arrhenius equation,²⁹ the average tunneling time through the pores is also estimated to be roughly in the order of $\sim \mu s$ at room temperature. The slight larger and almost flat binding energy curve of hydrogen inside the tube indicates that the inner space of the tube can hold hydrogen efficiently. Once hydrogen molecules diffuse into the tube, it can move back to outer region or diffuse along the tube. The inset of Fig. 4 shows the energy profile of hydrogen diffusion along the tube axis. The position of hydrogen along the tube is given relative to the center of the pore. There is a smaller diffusion barrier of about 2 kJ/mol, which is low enough for thermal diffusion at room temperature. The current simulation indicates that activating BNTs with such pore structures can make a full use of available surface area for hydrogen adsorption with higher binding energies.

A practical issue to address is how to make BNT into such activated forms. For carbon nanotubes, for instance, the chemical activation considered here may be achieved relatively easily. Recent high resolution transmission electron microscopy images show that vacancies are created and remain stable in graphite.²⁵ Structural defects including vacancies in carbon nanotube and graphite are generated by high-energy ion or electron bombardment, or during chemical processes.³⁰⁻³³ Oxygen molecules react with such defects in graphite, which leads to the formation of oxidized pits. Direct substitution of carbon by oxygen is also possible by wet chemistry applied to nanotubes.³⁴ Little is known about oxidation of BNTs, but similar methods used in CNTs can be applied for oxygenating BNTs. The formation energy of such

active pores can be estimated from the total energy calculations even though more accurate computation needs detailed information of true chemical reactions. For double-vacancy pores, for example, the formation energy can be given as

$$E_f = E_T(a\text{BNT}) + E_T(\text{B}_3\text{N}_3) - 2E_T(\text{O}_2) - E_T(\text{BNT}), \quad (1)$$

where $E_T(\dots)$ denotes the total energy of the system (\dots). For B_3N_3 cluster in Eq. (1), a hexagonal form similar to borazin less six hydrogen atoms is considered as a reference configuration. It is found that an energy of about 6 eV (or 8 eV if spin-polarization effect of O_2 is included) is required to create one double-vacancy pore with oxygen edge. Being an upper bound for the true formation energy, this estimation suggests that the activation should occur in highly nonequilibrium conditions as expected.

IV. SUMMARY

It is shown through *ab initio* computational simulations that activated BNTs can be good hydrogen storage media

operating at room temperature. The most efficient activation among the configurations considered here is the pore structure with oxygen edge. For pores of appropriate size, it is found that hydrogen can diffuse inside the tube, which leads to an increase of available adsorption sites for hydrogen and hence the storage capacity. This study demonstrates that introducing sufficient oxidized pores in BNTs is an effective method of activating BNTs, making them a strong candidate for hydrogen storages operating at elevated temperatures.

ACKNOWLEDGMENTS

This work was supported by the POSTECH BSRI Research Fund 2005 (Grant No. 1RB0510401) and by the Korea Research Foundation Grant funded by Korea Government (MOEHRD, Basic Research Promotion Fund) (Grant No. KRF-2005-070-C00041).

*Email address: jhish@postech.ac.kr

¹L. Schlaphbach and A. Züttel, *Nature* (London) **414**, 353 (2001).

²A. Zuttel, *Mater. Today* **6**, 24 (2003).

³A. Zuttel, D. Chartouni, L. Schlaphbach, and C. Nutzenadel, *Electrochem. Solid-State Lett.* **2**, 30 (1999).

⁴K. Murata, K. Kaneko, H. Kanoh, D. Kasuya, K. Takahashi, F. Kokai, M. Yudasaka, and S. Iijima, *J. Phys. Chem. B* **106**, 11132 (2002).

⁵T. Oku, I. Narita, A. Nishiwaki, and N. Koi, *Defect Diffus. Forum* **226-228**, 113 (2004).

⁶P. Dyson and J. McIndoe, *Angew. Chem., Int. Ed.* **44**, 5772 (2005).

⁷Q. Sun, Q. Wang, and P. Jena, *Nano Lett.* **5**, 1273 (2005).

⁸F. E. Pinkerton, B. G. Wicke, C. H. Olk, G. G. Tibbetts, G. P. Meisner, M. S. Meyer, and J. F. Herbst, *J. Phys. Chem. B* **104**, 9460 (2000).

⁹R. Yang, *Carbon* **38**, 623 (2000).

¹⁰A. Zuttel, C. Nutzenadel, P. Sudan, P. Mauron, C. Emmenegger, S. Rentsch, L. Schlaphbach, A. Weidenkaff, and T. Kiyobayashi, *J. Alloys Compd.* **330**, 676 (2002).

¹¹M. Hirscher *et al.*, *Appl. Phys. A: Mater. Sci. Process.* **72**, 129 (2001).

¹²The van't Hoff equation, describing the equilibrium pressure (p) of gas adsorption at temperature (T), is given as $\ln p = -\Delta H/k_B T + \Delta S/R$, where ΔH is the heat of adsorption, k_B Boltzmann constant, ΔS the change in entropy, and R is the gas constant. The equation is obtained by equating the free energies of adsorbed hydrogen and hydrogen at gas phase.

¹³S.-H. Jhi and Y. K. Kwon, *Phys. Rev. B* **69**, 245407 (2004).

¹⁴R. Z. Ma, Y. Bando, T. Sato, D. Golberg, H. W. Zhu, C. L. Xu, and D. H. Wu, *Appl. Phys. Lett.* **81**, 5225 (2002).

¹⁵R. Z. Ma, Y. Bando, H. W. Zhu, T. Sato, C. L. Xu, and D. H. Wu, *J. Am. Chem. Soc.* **124**, 7672 (2002).

¹⁶S.-H. Jhi and Y. K. Kwon, *Phys. Rev. B* **71**, 035408 (2005).

¹⁷J. W. Steed and J. L. Atwood, *Supramolecular Chemistry* (Wiley, Chichester, England, 2000).

¹⁸H.-J. Schneider and A. Yatsimirsky, *Principles and Methods in*

Supramolecular Chemistry (Wiley, Chichester, England, 2000).

¹⁹S.-H. Jhi, *Microporous Mesoporous Mater.* **89**, 138 (2006).

²⁰M. L. Cohen, *Phys. Scr.* **T1**, 5 (1982).

²¹D. SanchezPortal, P. Ordejon, E. Artacho, and J. M. Soler, *Int. J. Quantum Chem.* **65**, 453 (1997).

²²J. P. Perdew, K. Burke, and M. Ernzerhof, *Phys. Rev. Lett.* **77**, 3865 (1996).

²³Y. Kim, Y. F. Zhao, A. Williamson, M. J. Heben, and S. B. Zhang, *Phys. Rev. Lett.* **96**, 016102 (2006).

²⁴S.-H. Jhi, Y. K. Kwon, K. Bradley, and J. C. P. Gabriel, *Solid State Commun.* **129**, 769 (2004).

²⁵A. Hashimoto, K. Suenaga, A. Gloter, K. Urita, and S. Iijima, *Nature* (London) **430**, 870 (2004).

²⁶G. Vidali, G. Ihm, H.-Y. Kim, and M. W. Cole, *Surf. Sci. Rep.* **12**, 135 (1991).

²⁷C. M. Brown, T. Yildirim, D. A. Neumann, M. J. Heben, T. Genett, A. C. Dillon, J. L. Alleman, and J. E. Fischer, *Chem. Phys. Lett.* **329**, 311 (2000).

²⁸J. J. Zhao, A. Buldum, J. Han, and J. P. Lu, *Nanotechnology* **13**, 195 (2002).

²⁹The Arrhenius equation is commonly used in evaluating the diffusion or reaction rate. For tunneling time (τ), it has a form of $\tau = -\tau_0 \exp(-E_b/k_B T)$, where τ_0 is a prefactor, k_B Boltzmann constant, E_b the appropriate energy barrier, and T is the temperature. Here the prefactor is given as $\tau_0 = 1/\nu$ with the frequency ν obtained with harmonic approximation for a hydrogen molecule lying in the binding energy curve. The energy barrier comes directly from the binding energy curve shown in Fig. 4.

³⁰P. M. Ajayan, V. Ravikumar, and J.-C. Charlier, *Phys. Rev. Lett.* **81**, 1437 (1998).

³¹Y. Zhu, T. Yi, B. Zheng, and L. Cao, *Appl. Surf. Sci.* **137**, 83 (1999).

³²J. Hahn, H. Kang, S. Lee, and Y. Lee, *J. Phys. Chem. B* **103**, 9944 (1999).

³³C. Kiang, W. Goddard, R. Beyers, and D. Bethune, *J. Phys. Chem.* **100**, 3749 (1996).

³⁴K. Komatsu, M. Murata, and Y. Murata, *Science* **307**, 238 (2005).